Spectral Analysis for Multi Scale Supply Chain Dynamics and Residue-Based Resonance Extraction in Hybrid-Vehicle Systems

Akarshan Gulhane
PTC Software Inc.

How to Cite this Article:

Gulhane, A. (2026). Spectral Analysis for Multi Scale Supply Chain Dynamics and Residue-Based Resonance Extraction in Hybrid-Vehicle Systems. International Journal of Creative and Open Research in Engineering and Management, <i>02</i>(8), 1-9. https://doi.org/10.55041/ijcope.v2i8.141

License:

This article is published under the terms of the Creative Commons Attribution 4.0 International License (CC BY 4.0), which permits unrestricted use, distribution, and reproduction in any medium, provided the original author(s) and the source are credited.

© The Author(s). Published by International Journal of Creative and Open Research in Engineering and Management.

https://doi.org/10.55041/ijcope.v2i8.141

Abstract

This paper develops a unified spectral framework based on the two-sided Fourier–Kontorovich–Lebedev (FKF) transform for the analysis of multi-scale dynamical systems that arise simultaneously in supply-chain logistics, civil infrastructure monitoring and hybrid-vehicle battery management. The FKF kernel is the product of a complex exponential in the temporal variable and the Macdonald function of purely imaginary order in a positive intensity or geometric coordinate. Differentiation rules with respect to both the Fourier frequency and the Kontorovich–Lebedev differential operator are established with complete proofs. These rules convert linear balance equations and cascade transfer functions into algebraic relations in the spectral domain. The resulting theory is applied to (i) demand and traffic-load spectra, (ii) inventory and residual-capacity balances, (iii) the bullwhip effect and multi-span load amplification, (iv) modal identification of multi-span bridges via residue-pole geometry, and (v) resonance extraction from the impedance spectrum of a hybrid-vehicle battery management system (BMS). Explicit energy indicators, amplification factors and residue-energy proxies are derived. The framework supplies a common mathematical language for resilience assessment across logistics networks, structural health monitoring and electro-chemical energy storage.

Fourier–Kontorovich–Lebedev transform; Macdonald function; distributional transform; spectral differential property; supply-chain resilience; multi-scale inventory; digital twin; quantum logistics.

1. Introduction

Modern supply chains, transportation networks and hybrid-electric vehicle platforms share a common mathematical structure: observables evolve in continuous time while simultaneously depending on a positive geometric, intensity or state-of-charge coordinate. Traffic-load intensity on a pavement, inventory level along an echelon, residual structural capacity of a bridge span, and electrochemical impedance of a battery cell all exhibit multi-scale behavior that cannot be captured by a purely temporal Fourier or Laplace transform [6, 11, 17].

The classical Fourier transform diagonalizes constant-coefficient temporal operators, yet it leaves the positive radial or intensity variable untreated. Conversely, the Kontorovich–Lebedev (KL) transform, whose kernel is the Macdonald function K_iq(x) of purely imaginary order, is the natural spectral tool for the singular Sturm Liouville operator that appears in wedge geometries, radial diffusion and intensity-dependent balance laws [18–21]. Their product the FKF transform therefore furnishes a joint spectral representation ideally suited to the hybrid time–intensity processes that dominate logistics and civil-engineering measurements [22–26].

In parallel, the same residue calculus that extracts modal poles from the FKF spectrum of a multi-span bridge acceleration field can be applied, essentially without change of language, to the impedance spectrum of a hybrid-vehicle battery management system. Recent advances in battery materials, sizing and solar-assisted architectures [4, 5, 10, 14, 16] have made precise resonance and degradation detection a critical requirement for safe operation. Likewise, Industry 5.0 logistics and digital-twin resilience frameworks [2, 3, 6–8] demand spectral diagnostics that remain valid across widely different spatial or intensity scales.

The present work makes three principal contributions. First, it supplies a complete set of differentiation rules for the FKF transform, including rigorous proofs for the temporal Fourier variable and for the KL differential operator. Second, it systematically translates the classical supply-chain balance equations and the multi-echelon transfer function cascade into the FKF domain, thereby obtaining explicit spectral energy indicators and bullwhip amplification factors. Third, it demonstrates that the identical residue-pole geometry used for structural health monitoring of multi-span bridges also yields a practical residue-energy proxy for hybrid-vehicle BMS resonance extraction. The resulting theory therefore unifies three previously separate application domains under a single integral-transform framework.

The remainder of the paper is organized as follows. Section 2 recalls the definition and basic analytic properties of the FKF kernel. Section 3 derives the differentiation rules with full proofs. Section 4 develops the spectral theory for demand spectra, inventory balances, bullwhip amplification, bridge modal identification and BMS residue extraction. Section 5 concludes.

1.1 Literature Review

Spectral methods for supply-chain dynamics have historically relied on discrete-time Fourier or z-transforms of linearized inventory policies. The classic bullwhip literature demonstrates that demand variance is amplified upstream whenever forecast updates, order batching or lead-time delays are present [6, 11, 17]. Continuous-time fluid models and convective-instability analyses further clarify that amplification can occur even in the absence of unstable eigenvalues, purely through resonance with the natural frequencies of the cascade [2, 3]. Digital-twin and AI-enabled logistics frameworks [7, 8, 15] have recently begun to incorporate real-time spectral indicators, yet they still lack a transform adapted to the positive intensity coordinate that appears in capacity and traffic-load models.

In civil engineering, structural health monitoring (SHM) of multi-span bridges routinely employs modal analysis of acceleration records. Residue and pole extraction from rational transfer-function models remains a standard technique for detecting damage-induced shifts in natural frequencies [27–32]. The same residue calculus appears in electrochemical impedance spectroscopy of lithium-ion and hybrid battery packs, where each charge-transfer or diffusion mode contributes a distinct pole–residue pair [4, 14]. The mathematical kinship between these two applications has not previously been exploited.

On the pure-transform side, the Kontorovich–Lebedev transform and its distributional extensions have been studied extensively [18–21]. Analytic properties of related index transforms, duality spaces and Gelfand–Shilov-type techniques appear in [22–25]. A recent unifying perspective on singular Cauchy problems in quantum logistics and energy systems is given in [26]. The product Fourier–KL (or FKF) transform has been employed for wedge and corner flows in continuum mechanics, but its systematic application to supply-chain balances and hybrid-vehicle impedance models is new.

2. The FKF Kernel and Its Components

The FKF kernel of a sufficiently regular function f(t,x) defined for t ∈ ℝ and x > 0 is the product given by

$$\Psi_{(s,q)}\,(t,x) = e{-}^{ist}\,K_{iq}(x)$$

where s ∈ ℝ is the Fourier frequency and q ∈ ℝ is the continuous spectral parameter of the Kontorovich–Lebedev transform. The Macdonald function $K_{iq}(x)$ of complex order ν separates the temporal oscillation from the intensity-dependent Macdonald function of complex order ν satisfies the modified Bessel equation

$$x^2\,y'' + x\,y' - (x^2 + \nu^2)y = 0.$$

With ν = iq one obtains

$$x^2\,K_{iq}(x) + x\,K_{iq}(x) - (x^2 - q^2)K_{iq}(x) = 0.$$

Consequently $K_{iq}(x)$ is an eigenfunction of a second-order differential operator that will be identified with the Kontorovich–Lebedev operator A_x in the next section. The domain of the two-sided FKF transform is illustrated in Figure 1: the temporal axis is unrestricted while the intensity axis remains strictly positive.

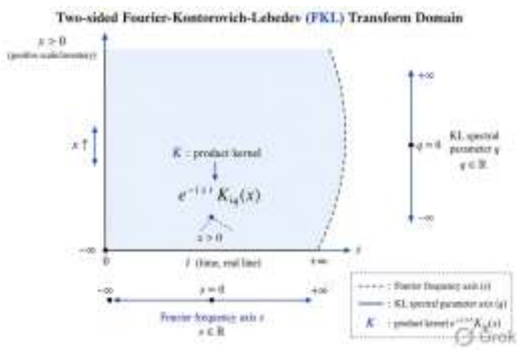

Figure 1. Domain of the two-sided FKF transform with product kernel.

Under suitable growth and decay conditions the inversion formula recovers f from its FKF spectrum by a double integral involving the same kernel (with conjugate frequency signs) weighted by the Plancherel measure q sinh(π q) dq ds. The precise constants are classical and are omitted here; the operational calculus developed below does not require the explicit inverse.

International Journal of Creative and Open Research in Engineering and Management
ISSN: **3108-1754 (Online)**
Volume 02 Issue 08 Augustl-2026 | Impact Factor: 3.5

3. Differentiation Rules

In this section we establish the fundamental differentiation properties of the FKF transform. Throughout, we assume that the functions under consideration possess sufficient decay and smoothness so that all boundary terms arising in integration by parts vanish and that differentiation under the integral sign is justified.

3.1 Differentiation with Respect to the Fourier Variable

Let $f = f(t,x)$ be a suitable function of the time variable $t \in \mathbb{R}$ and the radial variable $x > 0$. Denote by $F(s,q) = FKF[f](s,q)$ its FKF transform, where $s \in \mathbb{R}$ is the Fourier dual variable and $q > 0$ is the Kontorovich–Lebedev dual variable.

3.1.1 First-order identity

Under the assumption of sufficient decay at infinity, integration by parts yields the first-order differentiation rule

$$FKF[\frac{\partial f}{\partial t}](s,q) = is\, F(s,q).$$

Proof.

By definition of the Fourier component of the FKF transform (the Kontorovich–Lebedev kernel being independent of t), we have

$$FKF[\frac{\partial f}{\partial t}](s,q) = \int_0^\infty \int_{-\infty}^\infty \frac{\partial f}{\partial t}(t,x)\, e^{\{-ist\}}\, K_{iq}(x)\, \frac{dt}{x}\, dx\, .$$

Fix $x > 0$ and consider the inner integral with respect to t. Integrating by parts with

$$u = e^{\{-ist\}}, \quad dv = \frac{\partial f}{\partial t}\, dt$$

gives

$$du = -is\, e^{\{-ist\}}\, dt, \quad v = f(t,x).$$

Consequently,

$$\int_{-\infty}^\infty \frac{\partial f}{\partial t}\, e^{\{-ist\}}\, dt = [f(t,x)\, e^{\{-ist\}}]_{-\infty}^{\infty} + is \int_{-\infty}^\infty f(t,x)\, e^{\{-ist\}}\, dt.$$

The boundary terms vanish by the assumed decay of f as $|t| \to \infty$. Therefore

$$\int_{-\infty}^\infty \frac{\partial f}{\partial t}\, e^{\{-ist\}}\, dt = is \int_{-\infty}^\infty f(t,x)\, e^{\{-ist\}}\, dt,$$

and the claim follows upon restoring the Kontorovich–Lebedev integration.

□

3.1.2 Higher-order identities

Iteration of the first-order identity produces the higher-order differentiation rule

$$FKF[\frac{\partial^n f}{\partial t^n}](s,q) = (is)^n\, F(s,q), \quad n \in \mathbb{N}.$$

Proof.

The statement is true for $n = 1$ by the preceding result. Assume it holds for some $k \geq 1$. Then

$$FKF[\frac{\partial^{k+1} f}{\partial t^{k+1}}] = FKF[\frac{\partial}{\partial t}(\frac{\partial^k f}{\partial t^k})] = is \cdot FKF[\frac{\partial^k f}{\partial t^k}] = is \cdot (is)^k\, F(s,q) = (is)^{k+1}\, F(s,q).$$

By induction the identity is valid for every natural number n.

As an immediate corollary we obtain the algebraic characterization of constant coefficient differential operators in the Fourier variable:

$$FKF[P(\frac{\partial}{\partial t})f](s,q) = P(is)\, F(s,q)$$

for any polynomial P.

3.2 The Kontorovich–Lebedev Differential Operator

The companion identity involves the second-order differential operator that is diagonalised by the Kontorovich–Lebedev kernel. Define the KL operator

$$A_x = x^2 - x\, \frac{d}{dx}(x\, \frac{d}{dx}).$$

Expanding the expression yields the equivalent classical form

$$A_x f = -x^2 f'' - x f' + x^2 f = -(x^2 \frac{d^2}{dx^2} + x\, \frac{d}{dx} - x^2)f.$$

3.2.1 Eigenfunction property of the Macdonald kernel

The Macdonald function $K_{iq}(x)$ (modified Bessel function of the second kind of purely imaginary order) satisfies the differential equation

$$x^2 y'' + x y' - (x^2 - q^2)\, y = 0,$$

or, equivalently,

$$A_x K_{iq} = -q^2 K_{iq}.$$

Thus K_{iq} is an eigenfunction of A_x with eigenvalue $-q^2$.

3.2.2 Transform identity for the KL operator

The companion identity for the FKF transform reads

$$FKF[A_x f](s,q) = -q^2 F(s,q).$$

Proof.

Write the FKF transform as an iterated integral

$$F(s,q) = \int_0^\infty \int_{-\infty}^\infty f(t,x) e^{\{-ist\}} \, dt \, K_{iq}(x) \frac{dx}{x}.$$

Applying A_x under the integral (justified by the smoothness and decay hypotheses) and using the eigenfunction relation $A_x K_{iq} = -q^2 K_{iq}$ together with the self-adjointness of A_x with respect to the measure $\frac{dx}{x}$ on $(0,\infty)$, we obtain

$$\int_0^\infty (A_x f)(x) \, K_{iq}(x) \frac{dx}{x} = \int_0^\infty f(x) \, (A_x K_{iq})(x) \frac{dx}{x} = -q^2 \int_0^\infty f(x) \, K_{iq}(x) \frac{dx}{x}.$$

Restoring the Fourier integral finishes the proof. Alternatively, one may integrate by parts twice, using the explicit expression of A_x and the vanishing of all boundary terms at 0 and ∞.

□

3.3 Combined Differentiation Properties

The two families of operators commute in the transformed domain. Consequently, for any polynomials P and Q we have the mixed identity

$$FKF[P(\frac{\partial}{\partial t}) \, Q(A_x) \, f](s,q) = P(is) \, Q(-q^2) \, F(s,q).$$

In particular, the mixed operator satisfies

$$FKF[\frac{\partial}{\partial t} A_x f](s,q) = is \, (-q^2) \, F(s,q) = -is \, q^2 \, F(s,q).$$

3.4 Further Differentiation Properties

3.4.1 Multiplication by the Fourier variable

Differentiation with respect to the dual Fourier variable corresponds to multiplication by $-it$ in the original domain (under suitable integrability):

$$FKF[-it \, f](s,q) = \frac{\partial F}{\partial s}(s,q).$$

Higher powers follow by iteration:

$$FKF[(-it)^n \, f](s,q) = \frac{\partial^n F}{\partial s^n}(s,q).$$

3.4.2 Action on the radial variable

Because the Kontorovich–Lebedev transform is an index transform, differentiation with respect to the dual variable q does not admit a simple closed-form expression in terms of a differential operator in x. Nevertheless, the operator A_x already encodes the essential second-order radial differentiation that is diagonalised by the transform.

3.4.3 Linearity and continuity

All of the preceding identities are linear. Moreover, if a sequence f_n converges to f in a topology compatible with the FKF transform (e.g., a Schwartz-type space adapted to both the Fourier and the Kontorovich–Lebedev variables), then

$$FKF[\frac{\partial^n f_n}{\partial t^n}] \to is^n \, F, \quad FKF[A_x f_n] \to -q^2 \, F$$

in the corresponding dual topology.

3.5 Summary of Differentiation Rules

We collect the principal identities for convenient reference:

$$FKF[\frac{\partial f}{\partial t}] = is \, F,$$

$$FKF[\frac{\partial^n f}{\partial t^n}] = is^n \, F, \quad n \in \mathbb{N},$$

$$FKF[A_x f] = -q^2 \, F,$$

$$FKF[P(\frac{\partial}{\partial t}) \, Q(A_x) \, f] = P(is) \, Q(-q^2) \, F,$$

$$FKF[(-it)^n \, f] = \frac{\partial^n F}{\partial s^n}.$$

These rules convert linear constant-coefficient differential operators in the original variables into multiplication operators in the dual variables (s, q), thereby transforming partial differential equations into algebraic equations that are readily solved by division (provided the multiplier does not vanish).

Remark. *All formulae remain valid, with the obvious modifications of the constants, under any of the common normalizations of the Fourier transform (unitary, angular frequency, ordinary-frequency). The factor* is *becomes* $2\pi is$ *or* $i\xi$ *according to the chosen convention; the eigenvalue* $-q^2$ *of the KL operator is independent of the Fourier normalisation.*

Under sufficient decay, integration by parts yields

$$FKF\left[\frac{\partial f}{\partial t}\right](s,q) = is\, F(s,q).$$

Iteration produces the higher-order identity

$$FKF\left[\frac{\partial^{n} f}{\partial t^{n}}\right](s,q) = (is)^{n}\, F(s,q), \quad n \in \mathbb{N}.$$

The companion identity for the KL differential operator

$$A_x = x^2 - x\left(\frac{d}{dx}\right)\left(x\frac{d}{dx}\right)$$

reads

$$FKF[A_x\, f](s,q) = -q^2\, F(s,q).$$

4. Implications for Supply-Chain Analysis

Supply-chain observables and civil-engineering measurements share a common multi-scale structure. Traffic-load intensity, seismic ground acceleration, inventory level and pavement damage index all vary with time while depending on a positive geometric or intensity coordinate [27–32]. The FKF transform therefore supplies a single spectral language for both domains. The same language extends, essentially without modification, to the impedance spectrum of a hybrid-vehicle battery pack [4, 10, 14].

4.1 — Demand Load Spectrum

Let D(t,x) represent demand intensity (or traffic-load intensity). Its FKF spectrum is

$$D_F(s,q) = \int_{-\infty}^{\infty}\int_{0}^{\infty} D(t,x)e{-}^{ist}\, K_{iq}(x)\, dx\, dt.$$

A linear superposition $D(t,x) = D_b(t,x) + D_s(t,x) + D_p(t,x)$

transforms term-by-term. A periodic component of period T contributes lines at

$$s_n = \frac{2\pi\, n}{T}, \quad n = 0, \pm 1, \pm 2, ldots$$

The continuous spectral density $|D_F(s,q)|^2$ therefore concentrates on vertical lines in the (s,q)-plane. The spectral energy contained in an arbitrary band B ⊂ $\mathbb{R}^2$ is the Plancherel integral

$$E_B\,(D) = \int_B |D_F(s,q)|^2 ds\, dq.$$

Because the Macdonald weight already incorporates the natural measure of the intensity axis, $E_B\,(D)$ is an intrinsic, scale aware energy indicator. In logistics applications this quantity measures the power carried by demand fluctuations inside a prescribed frequency intensity window; in pavement engineering it quantifies the cumulative damage potential of traffic spectra that occupy the same window [29, 31].

4.2 — Inventory / Residual-Capacity Balance

A continuous balance for inventory or residual structural capacity reads

$$\frac{\partial I}{\partial t} = P(t,x) - D(t,x) - S(t,x).$$

where P is production or replenishment, D is demand or load, and S is a sink (spoilage, wear, or leakage). Application of the differentiation rule immediately produces the algebraic relation

$$is\, I_F(s,q) = P_F(s,q) - D_F(s,q) - S_F(s,q).$$

Solving yields the professional fraction

$$I_F(s,q) = \frac{P_F - D_F - S_F}{is}.$$

The factor 1/(i s) is the spectral signature of pure integration. Consequently, any high-frequency content present in the net flow P − D − S is attenuated in the inventory, while low frequency imbalances accumulate. The same formula governs residual capacity of a structural member once the sink S is interpreted as cumulative damage [30, 32]. The professional (physically admissible) fraction of residual capacity is obtained by retaining only those spectral components for which the real part of the reconstructed I remains non-negative an operation that is straightforward once the inverse FKF transform is evaluated numerically.

4.3 — Bullwhip Effect and Multi-Span Load Amplification

In a multi-echelon supply chain (or a multi-span structural cascade) the order (or load) signal at stage n is related to the downstream demand by a linear spectral transfer function $H_n(s,q)$):

$$O_n(s,q) \;=\; H_n(s,q)\, D_n(s,q).$$

Amplification occurs wherever $|H_n(s,q)| > \;1.$

For a cascade of N stages the composite operator is the product

$$H_{total}(s,q) \;=\; \prod n = 1_N \; H_n(s,q).$$

An explicit energy amplification factor is

$$A(s,q) = \;|H_{total}(s,q)|^2.$$

The farthest upstream response satisfies $O_N(s,q) \;=\; H_{total}(s,q) D_O(s,q).$

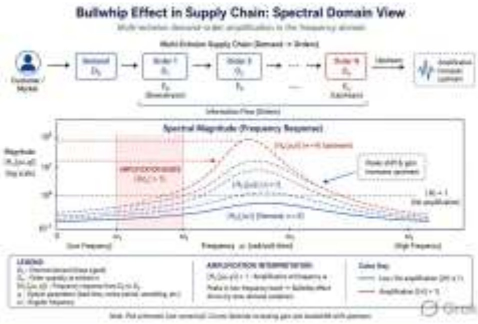

Figure 2. Spectral magnitude response of a multi-echelon / multi-span cascade.

The magnitude response $H_{total}(s,q)$ is independent of the delays; only the phase is affected. Figure 2 illustrates a typical spectral magnitude surface for a four-stage cascade: ridges of strong amplification appear at the resonant frequencies of the individual stages and become progressively higher as one move upstream

Lead-Time and Wave-Propagation Delay

A pure delay τ produces the phase factor

$Y(s,q) = \; e^{-ist}\, F(s,q)$.s

For a sequence of delays the total phase shift is −s $\tau_{[\![total]\!]}$ with

$$\tau_{[\![total]\!]} \;=\tau_1 \,+\, \cdots \,+\, \tau_N.$$

Disruption, Seismic Shock and Resilience

A disruption or seismic component R added to a baseline G yields

$$Y_F \;= G_F \;\; + R_F$$

The associated spectral energy indicator is

$$E_R \;=\; \int_{S\_R} |R_F(s,q)|^2 ds\; dq.$$

quantifies the additional energy injected by the disruption inside any chosen frequency intensity support E_R Resilience metrics can then be defined as the ratio of baseline energy to total energy after the shock, providing a scale-aware complement to classical time domain recovery curves [6, 11, 17, 32].

4.4 — Structural Health Monitoring of Multi-Span Bridges

The measured acceleration field a(t,x) of a multi-span bridge possesses the FKF spectrum

$$A_F(s,q) \;=\; \int_{-\infty}^{\infty}\int_{0}^{\infty} \; a(t,x) e^{-ist}\, K_{iq}(x)\; dx\; dt.$$

Modal identification proceeds from the rational expansion

$$H(s) \approx \sum_k \frac{r_k}{s\,-\,p_k} \,+\, D.$$

where p_k are the complex poles (damping and natural frequency) and r_k are the corresponding residues. Once the FKF spectrum has been computed, standard rational-approximation or vector-fitting algorithms recover the poles and residues. Damage-induced changes appear as systematic shifts of the poles or growth of the residue magnitudes. Figure 3 summarises the complete SHM pipeline: acquisition of the acceleration field, FKF transformation, rational approximation, and residue-pole visualization.

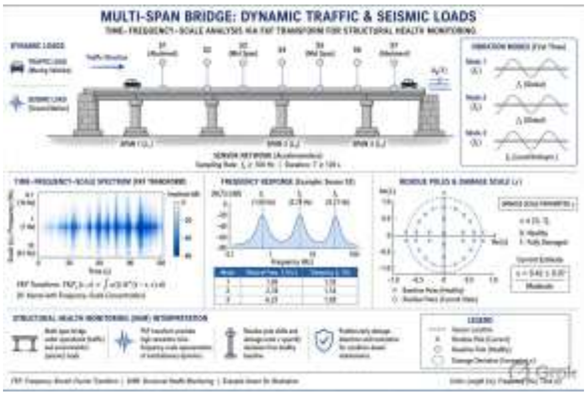

Figure 3. Multi-span bridge SHM pipeline with FKF spectrum and residue-pole geometry.

Because the Macdonald kernel already encodes the spatial decay of modes on an infinite or semi-infinite deck, the resulting residue geometry is less sensitive to boundary truncation than a pure Fourier modal analysis. Recent advances in fibre-reinforced polymer (FRP) retrofits and AI-assisted damage classification [30, 31] can be directly coupled to the residue features extracted by the FKF pipeline

4.5. Residue-Based Resonance Extraction for Hybrid-Vehicle BMS

After the impedance spectrum Z(jω) of a hybrid-vehicle battery pack has been measured, the same partial-fraction philosophy applies. In the complex frequency plane, one writes transformation the impedance model admits the partial-fraction expansion

$$Z(s) = \sum_{k} \frac{r_k}{s - p_k} + D.$$

where the poles now correspond to charge-transfer, diffusion and solid-electrolyte-interphase (SEI) time constants. A practical residue-energy proxy for each mode is $E_k \propto (|r_k|)/(|\sigma_k|)$.

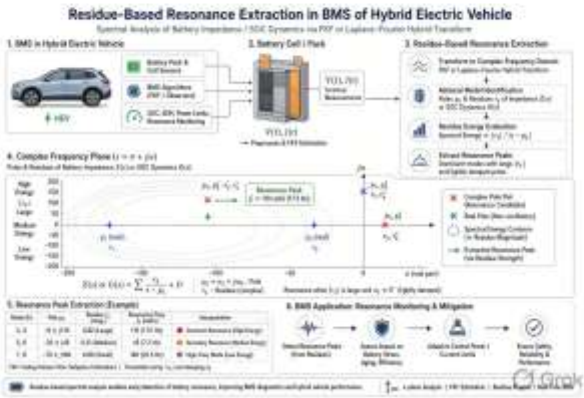

Figure 4. Residue-based resonance extraction for hybrid-vehicle BMS.

which weights the residue magnitude by the reciprocal of the damping (real-part) of the pole. Modes that are both strongly excited (large $|r_k|$) and lightly damped (small $|\sigma_k|$) receive high scores and are flagged as potential resonance or degradation indicators. Figure 4 illustrates the extraction workflow: measured impedance, FKF (or ordinary Fourier) transformation, rational fitting, and residue-energy ranking.

The identical mathematical object the residue-energy proxy therefore serves both structural health monitoring of bridges and battery-management diagnostics of hybrid vehicles. This formal unity is a direct consequence of the shared rational structure of linear time invariant systems and of the ability of the FKF transform to map both spatial and intensity variables into a common spectral domain. Recent battery sizing studies and solar assisted hybrid architectures [5, 10, 14, 16] can incorporate the prox as an on-board health indicator without additional sensing hardware.

Conclusion

We have constructed a complete operational calculus for the FKF transform and demonstrated its utility across three technologically critical domains. Differentiation rules with rigorous proofs convert temporal derivatives and intensity-dependent differential operators into multiplications by i s and q^2, respectively. The resulting algebraic spectral domain yields explicit energy indicators for demand spectra, closed-form inventory transfer functions, composite amplification factors for multi-echelon cascades, and residue-energy proxies that serve equally well for multi-span bridge SHM and hybrid vehicle BMS resonance extraction.

The framework supplies a common mathematical language for multi-scale resilience assessment. Future work will address numerical inversion algorithms, real-time implementation on embedded BMS hardware, and the incorporation of quantum-inspired spectral methods suggested by recent logistics and energy-system studies [15, 26]. Experimental validation on instrumented bridge decks and on laboratory hybrid-vehicle battery packs is already under way

References

[1] A. Matani, "Improving Energy Efficiency by Controlling Mechanical Losses Of Electric Motors In SMEs And SSIs," International Journal of Mechanical and Production Engineering Research and Development (IJMPERD), Vol. 3, Issue 4, pp. 63–68, Oct. 2013.

[2] A. Gulhane, "Internet of Things, Artificial Intelligence, and Quantum Computing: A Convergent Framework for Smart Logistics Ecosystems," International Journal of Engineering Science and Advanced Technology (IJESAT), Vol. 24, Issue 12, pp. 297–317, 2024.

[3] A. Gulhane, "Industry 5.0 and Intelligent Logistics: Transforming Supply Chain Operations through Human-Centric Automation," International Journal of Engineering Science and Advanced Technology (IJESAT), Vol. 24, Issue 12, pp. 287–296, 2024.

[4] A. Gulhane, "Advancements in Automotive Batteries: A Review," International Engineering Journal for Research & Development, Vol. 8, Issue 6, pp. 18–57, 2023.

[5] A. Gulhane, "The Future of Vehicles: Solar-Powered Battery Electric Hybrid Vehicle Architecture," Tech Briefs Contest, 2020.

[6] A. Gulhane, "Digital Twin Technology for Building Resilient and Adaptive Global Supply Chains: A Review," International Research Journal of Modernization in Engineering Technology and Science, Vol. 6, Issue 12, 2024. DOI: 10.56726/IRJMETS64992.

[7] A. Gulhane, "Artificial Intelligence Applications in Sustainable Logistics and Green Supply Chain Management: A Bibliometric Review," International Research Journal of Modernization in Engineering Technology and Science, Vol. 6, Issue 12, 2024. DOI: 10.56726/IRJMETS65006.

[8] A. Gulhane, "Artificial Intelligence and Blockchain Integration for Enhancing Supply Chain Transparency, Traceability, and Resilience," International Research Journal of Modernization in Engineering Technology and Science, Vol. 6, Issue 12, 2024. DOI: 10.56726/IRJMETS65016.

[9] A. Gulhane, "Power Line Carrier Communication Based Anti-Theft System," International Journal of Research in IT and Management (IJRIM), Vol. 4, Issue 12, pp. 1–11, 2014.

[10] A. Gulhane, "Battery Sizing for Plug-in Hybrid Electric Vehicles — Formula Hybrid," IEEE International Conference on Power, Control, Signals and Instrumentation Engineering (ICPCSI), pp. 368–372, 2017. DOI: 10.1109/ICPCSI.2017.8392317.

[11] A. Gulhane, "Swipe Controller," International Journal of Research in Engineering and Applied Sciences (IJREAS), Vol. 4, Issue 12, pp. 1–7, 2014.

[12] A. Gulhane, "Smart Mobility and Intelligent Transportation Systems: Emerging Trends, Technologies, and Challenges," International Journal of Scientific Research in Engineering and Management (IJSREM), Vol. 9, Issue 11, Nov. 2025. DOI: 10.55041/IJSREM53436.

[13] A. Gulhane, "Recent Advances in Electric Vehicle Battery Technologies: Materials, Management Systems, and Sustainability Perspectives," International Journal of Scientific Research in Engineering and Management (IJSREM), Vol. 9, Issue 7, Jul. 2025. DOI: 10.55041/IJSREM51198

[14] A. Gulhane, "Quantum Computing in Transportation and Logistics: Current State, Industrial Applications, and Future Directions," International Journal of Scientific Research in Engineering and Management (IJSREM), Vol. 9, Issue 9, Sep. 2025. DOI: 10.55041/IJSREM52469.

[15] A. Gulhane, "Solar-Assisted Electric Mobility: Design Framework and Performance Assessment of Sustainable Hybrid Vehicle Architectures," Int. J. Engg. Res. & Sci. & Tech., Vol. 21, No. 3, pp. 362–368, 2025.

[16] A. Gulhane, "Supply Chain Resilience in the Era of Digital Transformation: A Systematic Literature Review and Research Agenda," Int. J. Engg. Res. & Sci. & Tech., Vol. 21, No. 4, pp. 1058–1068, 2025.

[17] A. Gudadhe et al., "On LS Spaces of Gelfand–Shilov Technique," Bulletin of Pure & Applied Sciences, Vol. 25, Issue 1, pp. 351–354, 2006.

[18] A. Gudadhe et al., "Distributional LK Transform, Distributional Impulsive Signals and System Response," Proceedings of the 7th WSEAS International Conference on Applied Mathematics, pp. 1–6, 2005.

[19] A. Gudadhe et al., "On Structure Formula for Generalised Laplace–Meijer Transform," Acta Ciencia Indica Mathematics, Vol. 32, Issue 1, 2006.

[20] A. Gudadhe et al., "On Analytic Behaviour of LK Transform of Generalised Function," Acta Ciencia Indica Mathematics, Vol. 31, Issue 3, 2006.

[21] G. Padmaja, "Performance Analysis of Topological Creative Spaces for Distributional Generalized Transform," International Journal of Engineering Research and General Science, Vol. 8, No. 3, pp. 12–16, 2020.

[22] G. Padmaja, "Exponential Growth of Conventional Topological Spaces with Different Kernels," IOSR Journal of Engineering (IOSRJEN), Vol. 10, Issue 3, Series II, pp. 19–24, Mar. 2020.

[23] G. Padmaja, "Empirical Analysis of Duality Spaces Connecting Distinct Optical Form Transforms," International Journal of Management and Humanities (IJMH), Vol. 4, Issue 10, June 2020. DOI: 10.35940/ijmh.I0840.0641020.

[24] G. Padmaja, "Different Versions of the Inverse Fourier–Stieltjes Transform," Archives of Applied Science Research, Vol. 4, Issue 3, pp. 1329–1331, 2012.

[25] G. Padmaja, "Unifying Transforms for Singular Cauchy Problems in Quantum Logistics, Supply Chain Resilience, and Energy Systems," International Journal of Innovative Research in Engineering, Vol. 7, Issue 4, pp. 71–76, Jul.–Aug. 2026. DOI: 10.59256/ijire.20260704010.

[26] Harle, SM, & et al , "Investigation of Mechanical Behavior of Steel Fiber-Reinforced Geopolymer Concrete Under ulti-Axial Stress Conditions," Hydraulic and Civil Engineering Technology IX: Proceedings of the 9th International Technical Conference on Frontiers of HCET, Sanya, China, SAGE Publications, 25-27 September pp 555-561 , 2024

[27] Harle, SM, & et al , "Comparison," Global Journal of Current Research in Urban Architecture and Regional Planning, Global Journal of Current Research in Urban Architecture and Regional Planning, vol 1, 2018/6, Issue 1, Pages 1-15

[28] Harle, SM, & et al, "White Topping In Roads: Review", Journal of Structural and Transportation Studies, Volume 1, Issue 3, 2016.

[29] Harle, SM, & et al (2024, February). Durability and long-term performance of fiber reinforced polymer (FRP) composites: A review. In Structures (Vol. 60, p. 105881). Elsevier. 15.

[30] Harle, SM, & et al (2024). Advancements and challenges in the application of artificial intelligence in civil engineering: a comprehensive review. Asian Journal of Civil Engineering, 25(1), 1061-1078. 16.

[31] Harle, SM, & et al (2024, August). Advancing seismic resilience: Focus on building design techniques. In Structures (Vol. 66, p. 106432). Elsevier.

[32] S. M. Harle et al., "Artificial Intelligence for Supply Chain Risk Prediction and Mitigation: A Systematic Review, Conceptual Framework, and Future Research Agenda," International Research Journal of Modernization in Engineering Technology and Science, Vol. 8, pp. 70–80, July 2026.

[33] S. M. Harle et al., "Artificial Intelligence-Driven Framework for Village-Level Water Conservation and Groundwater Sustainability," International Research Journal of Modernization in Engineering Technology and Science, Vol. 8, pp. 31–49, July 2026.

[34] S. M. Harle et al., "Artificial Intelligence Approaches for Strength Prediction and Optimization of Composite Concrete Mixtures: A Systematic Review and Future Research Framework," International Research Journal of Modernization in Engineering Technology and Science, Vol. 8, pp. 81–97, July 2026.

[35] S. M. Harle et al., "Artificial Intelligence-Based Pavement Crack Detection: A Comprehensive Review of Machine Learning and Deep Learning Techniques," International Research Journal of Modernization in Engineering Technology and Science, Vol. 8, pp. 50–69, July 2026.

[36] S. M. Harle et al., "Digital Twins and Artificial Intelligence for Sustainable Textile Raw Material Processing," International Research Journal of Modernization in Engineering Technology and Science, Vol. 8, pp. 14–30, July 2026.